

# Hybrid Controller Based Solar-Fuel Cell Integrated UPQC for Power Quality Enhancement

Sravanthy Gaddameedhi\* , Koganti Srilakshmi\* , K. Krishna Jyothi \*\*   
G. Kalyani\*\* , Aryan\* , K. Sumanth \* , Aravindhababu Palanivelu\*\*\* 

\*Department of Electrical Engineering, Sreenidhi Institute of Science and Technology, Hyderabad, Telangana, 501301.

\*\*Department of Computer Science Engineering, Geethanjali College of Engineering and Technology, Hyderabad, Telangana, 501301.

\*\*\*Department of Electrical Engineering, Annamalai University, Annamalai Nagar, Tamil Nadu.

([sravanthi314@gmail.com](mailto:sravanthi314@gmail.com), [kogantisrilakshmi29@gmail.com](mailto:kogantisrilakshmi29@gmail.com), [kogantikrishnajyothi@gmail.com](mailto:kogantikrishnajyothi@gmail.com), [g.kalyani@gmail.com](mailto:g.kalyani@gmail.com), [Y.aaryan12@gmail.com](mailto:Y.aaryan12@gmail.com),  
[sumanthk@sreenidhi.edu.in](mailto:sumanthk@sreenidhi.edu.in), [aravindhababu@gmail.com](mailto:aravindhababu@gmail.com) )

‡

Corresponding Author: Sravanthy Gaddamedhi, Sreenidhi Institute of Science and Technology, Tel: +91-8919787765,  
[sravanthi314@gmail.com](mailto:sravanthi314@gmail.com).

*Received: 20.09.2021 Accepted:24.10.2021*

**Abstract:** This work introduces a fuzzy and integral sliding mode hybrid controller (FISMHC) for unified power quality conditioner (UPQC) with solar system (SS) integrated with fuel cell (FC) for enhancement of power quality in distribution networks. The SS and FC based UPQC consists of a series and a shunt active power filters, which are coupled back-to-back with a common dc link capacitor. The goals of the proposed UPQC with FISMHC (U-FISMHC) are: (1) maintenance of constant DC-link voltage with very low settling time without overshoot, (2) great performance while eliminating grid voltage fluctuations, and (3) reduction of harmonics both in source currents and load voltages. Further, this work investigates the performances of U-FISMHC on a distribution system with three different test cases involving changes in solar irradiation, supply voltages and loads, and compares the performances with those of proportional-integral controller (PIC), fuzzy logic controller (FLC) and sliding mode controller (SMC) for exhibiting the superior performances of the proposed controller.

**Keywords-** Power Quality, UPQC, pulse width modulation, fuzzy logic, THD, voltage sag and swell.

## 1. Introduction

Power quality (PQ) problems are raised due to the usage of large nonlinear loads, power electronics devices and integration of distributed generations in distribution networks. A small improvement in PQ significantly increases the lifetime and performances of utility equipment. Several FACTS devices are developed to overcome these PQ issues. UPQC is an important multifunctional FACTS device combining both DVRs and DSTATCOMs in minimizing the effects of harmonic currents, voltage sags/swells, and unbalanced loads. The effectiveness of UPQC in eliminating the PQ issues primarily depends on the design and choice of an appropriate controller.

The hybridization of both the series and shunt-active power filters (SAPF & SHAPF) was suggested for building

UPQC with a goal of providing compensation to voltage sags/swells, VAR, and harmonic currents. The method adapted a control scheme involving instantaneous power theory [1]. The design of UPQC involving both SAPF & SHAPF, and sliding mode controller for tracking the reference voltage was discussed. The dynamic voltage regulator was used as a SAPF and provided compensation during unbalanced voltage condition in addition to regulating the load voltage with minimum VA loading of the UPQC [2]. Fuzzy hysteresis band voltage and current control (CC) strategies were developed for UPQC with a view of providing compensation for harmonics and grid voltages [3]. The functionality of UPQC was modified to give equal sharing to both SAPF and SHAPF, thereby reducing the rating of SHAPF and the overall cost of UPQC [4]. An artificial neural network (ANN) based controller was outlined for performing CC for SHAPF of UPQC, wherein the ANN was developed off-line using the data of

classical proportional-integral controller (PIC) [5]. An optimal control strategy with linearized feedback for UPQC was developed with a goal of obtaining optimal voltage angle at load and minimizing the converter losses [6]. An exhaustive review was performed for presenting different UPQC configurations and various compensation schemes [7]. A differential evolution-based scheme for optimal placement of UPQC was suggested by considering multiple objectives of enhancing voltage / current profiles, minimizing the power loss and reducing the investment cost [8]. A fuzzy control scheme was suggested for a 3-level neutral point clamped inverter topology based UPQC for effectively mitigating source current harmonics and providing compensation for all voltage fluctuations [9]. The design aspects of PV integrated UPQC were discussed with a view of minimizing grid voltage and load current disturbances in addition to providing reactive and harmonic power compensation [10].

Integral plus sliding mode control (SMC) technique-based capacitor voltage regulator for UPQC was presented for maintaining constant DC-Link voltage with very low settling time and no overshoot [11]. The techniques adapted for harmonic analysis, mathematical modeling and mitigation techniques were exhaustively reviewed [12]. A scheme containing UPQC was suggested for a micro-grid comprising PV/Wind/Fuel cell/Battery systems with a view of addressing PQ related problem [13]. A harmonic mitigation scheme involving UPQC for induction furnace load at steel plant was developed and its performance was portrayed to be much better than that of distributed synchronous compensator [14]. The design of hybrid controller involving both SMC and instantaneous power theories for UPQC was carried out to minimize total harmonic distortions (THD) and grid voltage distortions [15]. An ANN controller, trained by Levenberg-Marquardt back-propagation algorithm, was developed for a 5-level UPQC with intend of eliminating mathematical operations and formation of reference signals, and also regulating the DC-link voltage [16]. A PV-tied UPQC with an improved LCL filter at SHAPF with part integral plus SMC was suggested for addressing voltage and current related PQ issues [17].

A fuzzy-ANN control for five-level UPQC was developed for minimizing the THD and improving the power factor [18]. The predator-prey based firefly optimization technique was applied in optimally designing SHAPF with an objective of minimizing THD [19]. The performances of various PWM strategies and different space vector PWM techniques were discussed [20]. PV and battery energy storage system based UPQC was suggested to minimize the THD and other grid voltage problems [21]. Various UPQC control strategies and algorithms were investigated in respect of PQ enhancement, and a versatile control strategy was suggested [22]. The performances of a 3phase H-bridge UPQC with D-STATCOM were investigated in view of minimizing the PQ issues [23]. DG feed multilevel UPQC was designed and comparative analysis was carried out with two-level converters [24]. The 3 phase 2 bus distribution system issues like real and reactive powers management, and THD reduction were

studied by connecting UPQC to different type of non-linear loads [25].

The comparison between P & O and PSO algorithms to get MPP for the PV system was studied for solar irradiation changes [26]. FDNE based method was developed based on online least square identification algorithm along with digital simulators [27]. High voltage isolated ACDC converters were developed based on the modular technology [28]. Experimental set-up of isolated boost full bridge DC-DC converter was investigated along with a set of low loss active snubber circuit [29]. Integration of renewable sources to micro grid for MPPT was studies with power management [30]. The enhanced most valuable player algorithm was used for solving multi-objective OPF [31]. Soccer league optimization was developed for transmission and distribution network load flow analysis [32].

In this article, a fuzzy and integrated sliding mode hybrid controller (FISMHC) has been developed for UPQC with solar system (SS) and fuel cell (FC) for minimizing the THD, improving the power factor, eliminating voltage fluctuations, and maintaining constant DC-link voltage with minimum settling time and without peak overshoot. The performances of the UPFC with FISMHC (U-FISMHC) have been studied on a 3-phase distribution system with different loads, PV-irradiations and supply voltages, and compared with those of the existing proportional integral controller (PIC), fuzzy logic controller (FLC), and sliding mode controller (SMC) to exhibit the superiority of the proposed scheme.

Configuration of the proposed SS-FC based UPQC is given in section-2. Controller of the proposed technique is designed in section-3. Test results are exhibited in section-4. Conclusions are drawn in section-5.

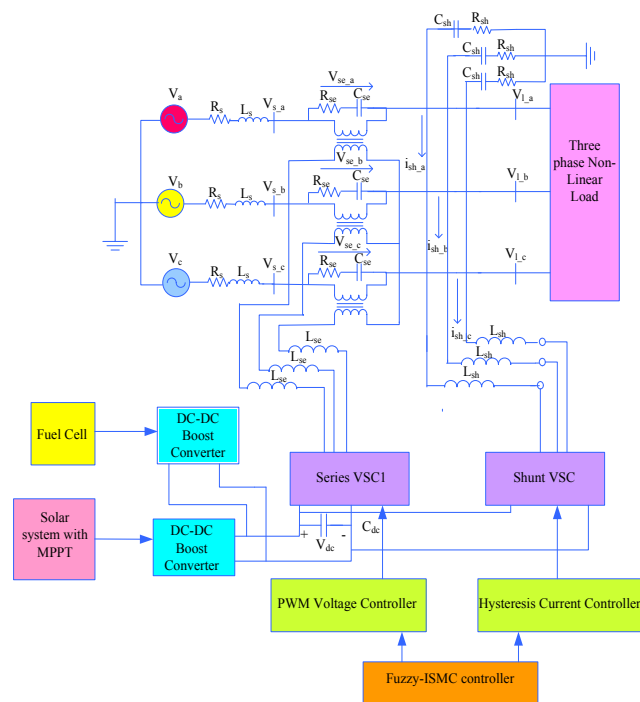


Figure 1: Configuration of proposed U-FISMHC

**2. Configuration of Proposed UPQC**

Fig.1 shows the arrangement of UPQC supported with FC and SS for a 3-phase distribution network. The SS and FC are connected to the UPQC's DC-link via boost converters. This work introduces a FISMHC for exploiting the properties of both fuzzy and integrated SMCs.  $V_a, V_b, V_c$  are the grid voltages for phases a, b, c respectively;  $V_{s_a}, V_{s_b}, V_{s_c}$  are source bus voltages for phases a, b, c respectively;  $V_l$  and  $i_l$  are load voltage and load current respectively;  $R_s$  and  $L_s$  are source resistance, and inductance respectively. UPQC is the combination of both SAPF and SHAPF. The prime function of SAPF is to minimize grid voltage fluctuations by injecting appropriate compensating voltage  $V_{se}$  through isolation transformer. The RLC filter comprises of a resistor  $R_{se}$ , an inductor  $L_{se}$  and a capacitor  $C_{se}$  at each phase.

The SHAPF, connected through resistances  $R_{sh}$ , interfacing inductances  $L_{sh}$ , and capacitances  $C_{sh}$  to the grid, intends to minimize current harmonics and maintain constant DC-link voltage with low settling time by injecting appropriate compensating current  $i_{sh}$ . The SS, FC specifications are furnished in Table-1, while the system and load specifications are given in Table-2.

Table1: SS and FC specifications

Device	Parameters	Values
PV panel (Sun Power SPR-215-WHT-U)	Rated Power	214.913 W
	Open circuit voltage	48.29 V
	Short circuit current	5.75 A
	Voltage/current at maximum power	39.82 V /5.43A
	Number of parallel cells	11
	Number of series cells	18
Fuel cell	Temperature	25 <sup>0</sup> c
	Total number of cells	65
	Efficiency of stack	55%
	Rate of air flow	300 IPM
	Fuel cell resistance	0.7183 Ω
	Resistance across the load	5 Ω
	voltage per one cell	1.138
	H <sub>2</sub>	99.661%
O <sub>2</sub>	59.41%	

Table 2: Network and UPQC parameters

Source	Voltage: 415V; Frequency: 50Hz; Resistance: 0.1Ω; Inductance: 0.15mH
Series compensator	Resistance: 1Ω; Inductance: 3.6 mH; Capacitance: 60 μf
Shunt compensator	Resistance: 0.001Ω; Inductance: 2.15 mH; Capacitance: 1 μf VSC hysteresis controller band: 0.01A

Dc-Link	Capacitance: 9400μf ; Voltage: 700V
Loads	Balanced 3 Φ rectifier load: R=30Ω, L=20mH. Unbalanced 3 Φ R-L load: R1=10Ω, L1=9.5mH, R2=20 Ω, L2=10.5mH, R3=15 Ω, L3=18.5mH. Induction Motor Load: LC = 400 mH, 50 μF, RL = 10 Ω, 100 mH.

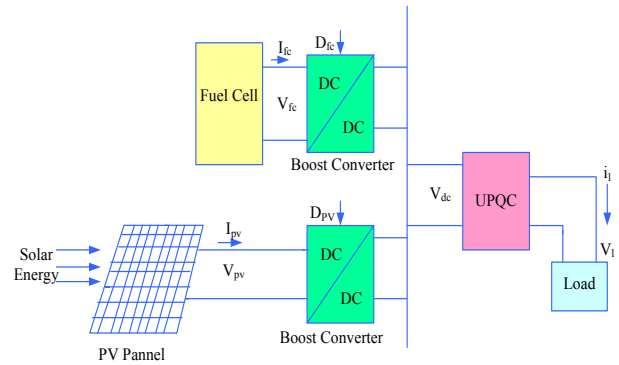


Figure 2: Components of External DC-Link support

2.1 External support for DC-Link

Fig. 2 illustrates the various components of the proposed UPQC scheme. SS with maximum power point tracking (MPPT) and FC are connected across the DC-link capacitor via DC-DC boost converters. The power balance equation for the proposed model is given by Eq. (1).

$$P_{PV} + P_{fc} - P_{LoadDC-Link} = 0 \tag{1}$$

2.1.1 Solar System (SS)

The solar PV system is employed for solar to electrical energy conversion. The SS consists of a PV panel, a boost converter and a MPPT controller as illustrated in Fig.3. The amount of electrical energy depends on solar radiation incident on PV cell. The MPPT is used to obtain maximum PV output voltage under the specified irradiance and temperature. The basic circuit of PV cell as in Fig. 4.

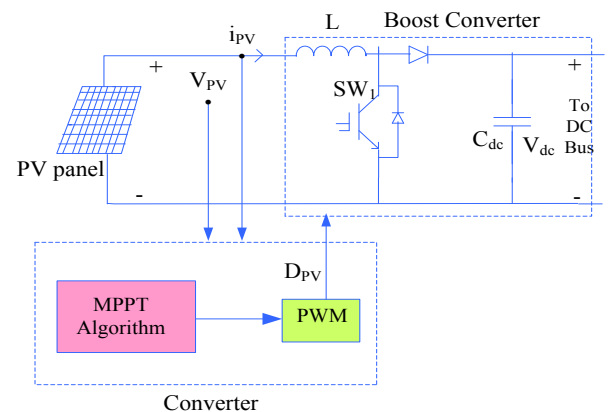


Figure 3: Solar system with controller

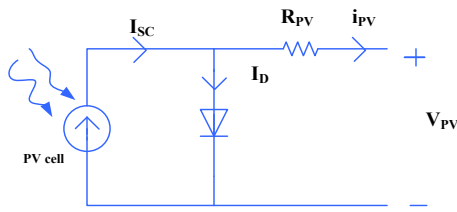


Figure 4: Model of PV solar cell.

The output power  $P_{PV}$  of PV panel can be evaluated by Eq. (2)

$$P_{PV} = V_{PV} * i_{PV} \tag{2}$$

Where,

$V_{PV}$ , and  $i_{PV}$  are the output voltage and current of the PV panel respectively.

In this work, the MPPT uses Perturb and Observes (P & O) method to control duty cycle (D) of the boost converter, as explained in Fig. 5. The necessary change in the duty cycle ( $\Delta D$ ) is estimated based on the variation in power ( $\Delta P$ ) and the variation in voltage ( $\Delta V$ ). If the power increases, the algorithm increases the voltage, and vice-versa.

2.1.2 Fuel cell (FC)

The fuel cell generates electrical energy from the chemical energy. The electrochemical reaction between  $H_2$  and  $O_2$  produces electricity. Multiple fuel cells are coupled to form a fuel cell stack to produce high voltage. The voltage level of the fuel cell is increased by boost converter. Fig. 6 shows the fuel cell controller with boost converter. The reference current  $i^{ref}_{dc}$  is estimated by minimizing the of DC-Link voltage error  $V_{dc, err}$  using a PIC by Eqs. (3) and (4).

$$V_{dc, err}(t) = V^{ref}_{dc} - V_{dc} \tag{3}$$

$$i^{ref}_{dc} = K_{p,1} V_{dc, err}(t) + K_{i,1} \int_0^t V_{dc, err}(t) dt \tag{4}$$

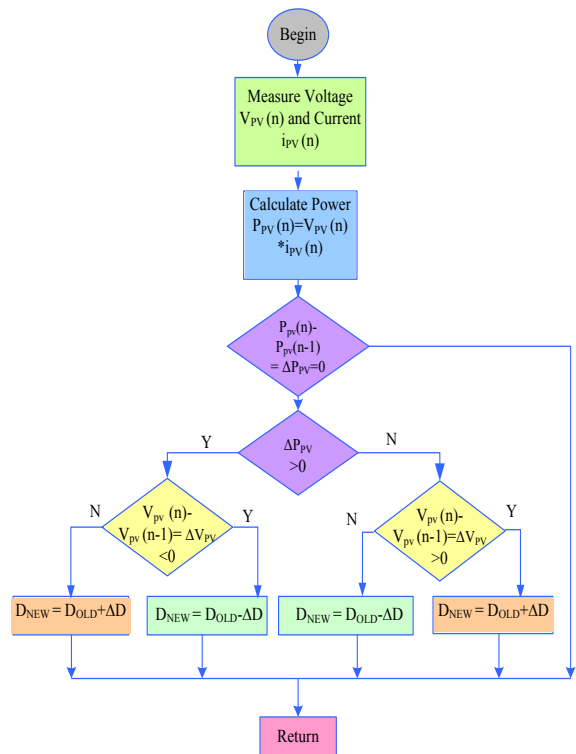


Figure 5: MPPT algorithm flow chart

The fuel cell error current reference  $i_{fc, err}^*$  is obtained from fuel cell error current  $i_{fc, err}$  by PI controller as given by Eq. (5).

$$i_{fc, err}^* = K_{p,2} i_{fc, err}(t) + K_{i,2} \int_0^t i_{fc, err}(t) dt \tag{5}$$

Here  $i_{fc, err}$  is the difference between reference DC-Link current  $i^{ref}_{dc}$  and fuel cell current  $i_{fc}$  as given by Eq. (6).

$$i_{fc, err}(t) = i^{ref}_{dc} - i_{fc} \tag{6}$$

The gains of both PI<sub>1</sub>, PI<sub>2</sub> controllers are heuristically chosen as  $K_{p1} = 1.5$ ,  $K_{i1} = 0.1$ ,  $K_{p2} = 1.477$  and  $K_{i2} = 3.077$ .

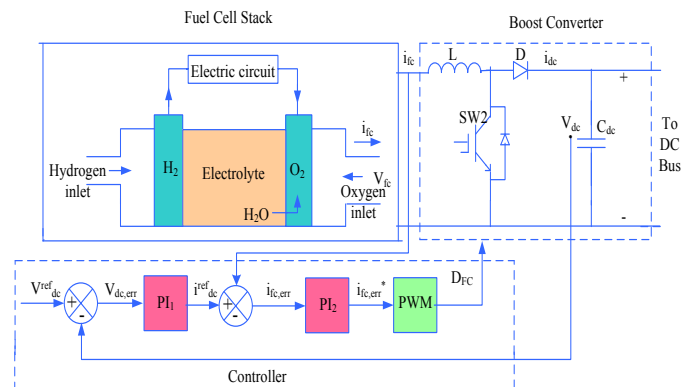


Figure 6: Fuel cell with controller

**3. Control Strategy**

During a fault, the voltage across DC-link capacitor varies. In order to make the system stable the voltage across the capacitor must be brought back to the original value. The switching control strategy for series and shunt VSCs are done by PWM voltage and PWM hysteresis CC with FISMHC. The proposed controlling structure consists of the following major parts:

**3.1 Shunt-VSC**

The role of the shunt-VSC is to reduce THD of current and regulate DC-link voltage. A FISMHC controller is used to maintain the constant DC-link voltage and generate reference currents. By extracting the active fundamental load current component, the proposed hybrid controller of SHAPF performs the load current compensation. The phasor locked loop (PLL) receives the grid voltages and provides the phase and frequency information, which are used to convert the load currents into the d-q-0 domain. After adding the d-q-0 component with DC link current, FISMHC is used to generate currents, which are then translated into the a-b-c domain for deriving reference injected currents ( $i_{sh}^{ref}$ ). In PWM hysteresis CC, these reference currents are compared with the sensed currents to produce the gating pulses ( $S_{a1}, S_{a2}, S_{b1}, S_{b2}, S_{c1}, S_{c2}$ ) for the shunt converter. Fig. 7 shows the shunt VSC Controller.

**3.1.1 Fuzzy Controller**

The FLC is used as DC link voltage regulator. The FLC receives error (E) and rate of change of error (CE) as inputs, and produces a duty cycle (D) as output. The error is given by  $E = V_{dc}^{ref} - V_{dc}^i$ ;  $i = 1, 2, 3, 4, 5, 6$ . Triangular membership functions are used for E, CE and D of the FLC as shown in Figs.8-10 respectively. The linguistic variables for E, CE and D are given as ‘‘POH’’ - Positive High, ‘‘POM’’ - Positive Medium, ‘‘POL’’- Positive Low, ‘‘ZO’’ – Zero, ‘‘NGL’’ - Negative Low, ‘‘NGM’’ – ‘‘Negative Medium, and ‘‘NGH’’ - Negative High. Fuzzy ‘‘IF-THEN’’ rules are created using these linguistic variables as given in Table 3. The accuracy can be improved by increasing the number of rules, but this inturn increases the data size, execution time and complexity of the control system.

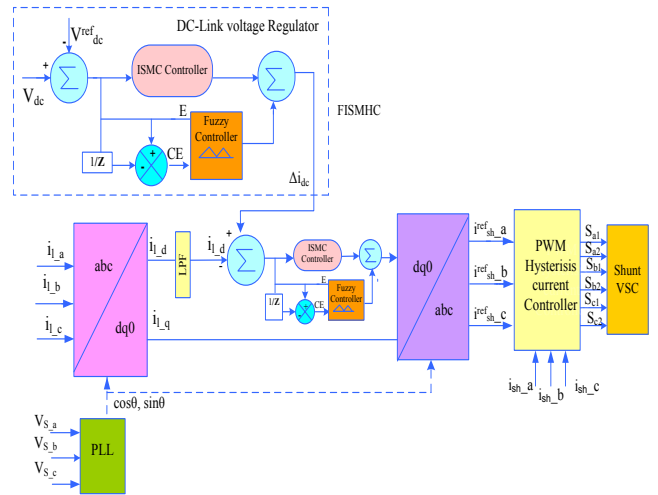


Figure 7: Shunt VSC Controller

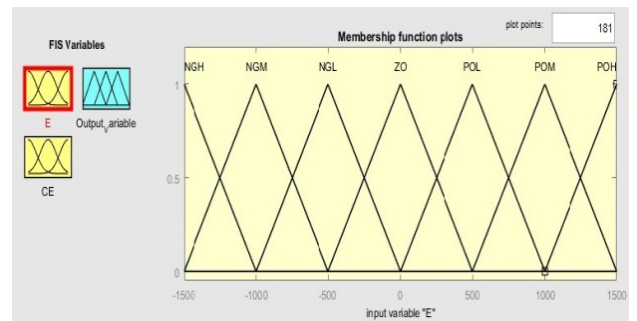


Figure 8: Membership function for error

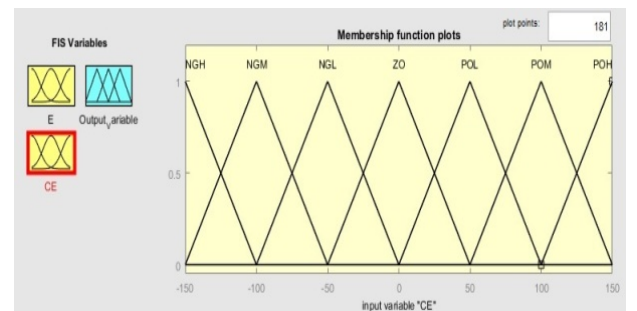


Figure 9: Membership function for change in error

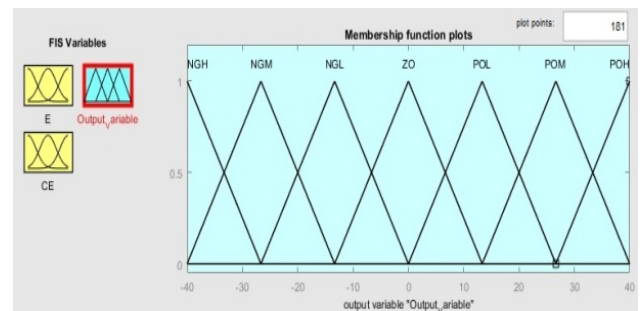


Figure 10: Membership function for duty cycle

Table 3: Fuzzy If –Then Rules

E	CE						
	POH	POM	POL	ZO	NGL	NGM	NGH
NGH	ZO	NGL	NGM	NGB	NGH	NGH	NGH
NGM	POL	ZO	NGL	NGM	NGH	NGH	NGH
NGL	POM	PSL	ZO	NGS	NGM	NGH	NGH
ZO	POH	PSM	PSL	ZO	NGL	NM	NGH
POL	POH	PSH	PSM	PSL	ZO	NGL	NM
POM	POH	PSH	PSH	PSM	PSL	ZO	NGL
POH	POH	PSH	PSH	PSH	PSM	PSL	ZO

3.1.2 ISMC Controller

SMC is popularly used for controlling power converters due to its speed. The prime motive behind the SMC is the surface specification, which is usually defined as a sliding surface. Here the control feature is to maintain the system within the surface. The SMC's three core design steps are 1) sliding surface proposal, 2) checking for existence of sliding mode surface, and 3) surface stability analysis.

The error  $e(n)$  is calculated by Eq. (7).

$$x_1 = V^{ref}_{dc} - V_{dc} = e(n) \tag{7}$$

The derivative of error is given by Eq. (8).

$$x_2 = \frac{1}{T} e(n) - e(n-1) \tag{8}$$

Here,  $T$  is time interval, and  $x_1$  and  $x_2$  are state-variables.

Eq. (9) gives the state equation.

$$\dot{x} = \begin{bmatrix} \dot{x}_1 \\ \dot{x}_2 \end{bmatrix} = \begin{bmatrix} 0 & 1 \\ 0 & 0 \end{bmatrix} \begin{bmatrix} x_1 \\ x_2 \end{bmatrix} + \begin{bmatrix} 0 \\ -k \end{bmatrix} \mu \tag{9}$$

The sliding mode plane and its state equation are represented by Eq. (10) and (11) respectively.

$$s = [C \quad 1] \begin{bmatrix} x_1 \\ x_2 \end{bmatrix} = Cx_1 + x_2 \tag{10}$$

$$\dot{s} = [C \quad 1] \begin{bmatrix} \dot{x}_1 \\ \dot{x}_2 \end{bmatrix} = C\dot{x}_1 + \dot{x}_2 \tag{11}$$

Power rate reaching law is given as,

$$\dot{s} = -L|s|^\alpha \text{sgn}(s) \tag{12}$$

Where,

$$\text{sgn}(s) = \begin{cases} 1 & \text{for } s > 0 \\ -1 & \text{for } s < 0 \end{cases} \tag{13}$$

The required control law  $\mu$  is calculated from Eqs. (9)-(13) as given below.

$$\mu = \frac{1}{K} [Cx_2 + L|s|^\alpha \text{sgn}(s)] \tag{14}$$

The control action is integrated with SMC [14] to obtain the modified control law as given in Eq. (15).

$$\mu = \frac{1}{K} [Cx_2 + L|s|^\alpha \text{sgn}(s)] + K_i \int_0^t e(\tau) d\tau \tag{15}$$

This method helps to enable  $V_{dc}$  to track  $V^{ref}_{dc}$  dynamically without steady-state error. It also works effectively even during load variations. The Simulink model of proposed hybrid controller is shown in Fig.12.

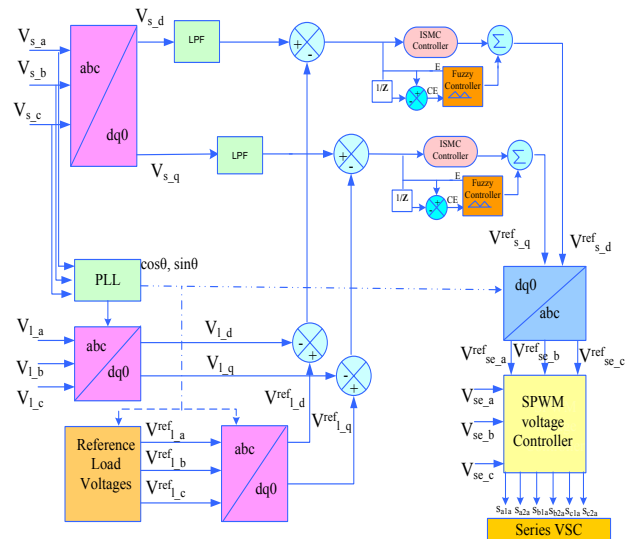


Figure 11: Series VSC controller

3.2 Series VSC

The SAPF injects suitable voltage to reduce grid voltage fluctuations and maintain constant load voltages. The control structure of SAPF is shown in Fig. 11. A PLL is used to extract the fundamental component of grid voltage, which is then used to generate the reference axis in d-q-0 domain. The data of phase and frequency retrieved from the PLL is used to produce the reference load voltage. The source, load, and reference voltages are then converted into d-q-0 domain. The difference between load and grid voltages is then passed through the FISMHC controller to produce  $V^{ref}_{se}$  in d-q-0 domain, which is later converted into a-b-c domain. The final output is given to the PWM voltage controller to produce the triggering pulses ( $S_{a1a}$ ,  $S_{a2a}$ ,  $S_{b1a}$ ,  $S_{b2a}$ ,  $S_{c1a}$ ,  $S_{c2a}$ ) for series VSC.

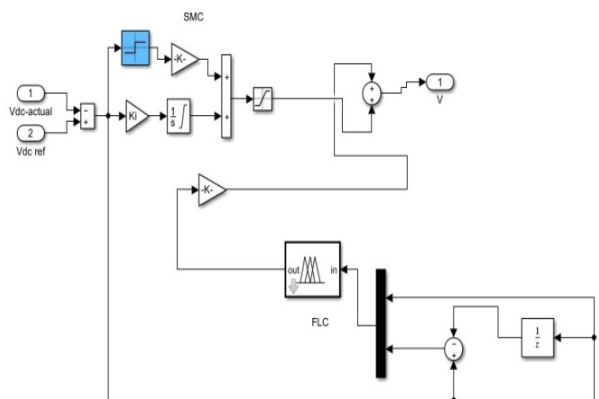


Figure 12: Simulink model of proposed FISMHC for DC-Link voltage control

#### 4. Results and Discussions

The simulations of U-FISMHC were carried out on a distribution network with specifications as given in Table-3. The Simulink model of the test system was designed in Matlab 2016a environment. The system was exposed to different PQ issues such as voltage fluctuations, unbalanced supply voltage, unbalanced load and solar irradiation, temperature variation. These PQ issues were considered as three different case studies as detailed in Table-4. The comparative analysis of proposed method is carried out with PIC, FLC and SMC.

Table 4: Test Cases Considered

Condition	Case-1	Case-2	Case-3
Balanced Supply	✓	✓	
Unbalanced Supply			✓
Voltage Sags/Swells, disturbance	✓	✓	
Constant irradiation at 1000 w/m2	✓		✓
Irradiance variation from 1000 w/m2 to 400 w/m2		✓	
Balanced 3 Φ full bridge rectifier load	✓	✓	
Unbalanced 3 Φ R-L load		✓	✓
Induction motor Load	✓		✓

The  $V_s$  was considered to be balanced for cases 1 and 2, and unbalanced for case 3. In addition, voltage sag and swell were considered in cases 1 and 2. The THD for both  $V_l$  and  $i_s$ , and the power factor were obtained for all the test cases with and without the proposed UPQC, and compared with those of existing PIC, FLC and SMC.

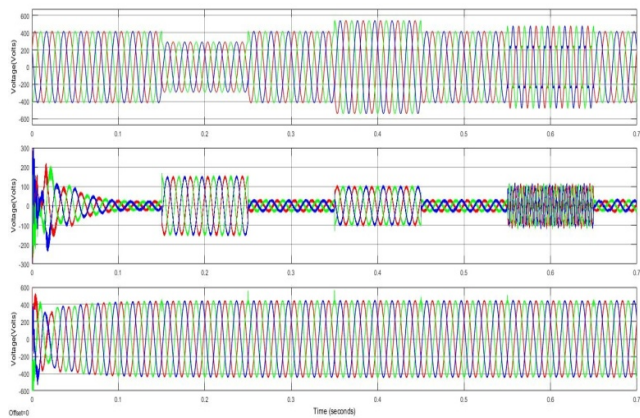
The sensed signals were source-voltage ( $V_s$ ), injected series voltage ( $V_{se}$ ), load-voltage ( $V_l$ ), load current ( $i_l$ ), injected shunt current ( $i_{sh}$ ), source current ( $i_s$ ), output current of PV panel ( $I_{PV}$ ), output voltage of PV panel ( $V_{PV}$ ), DC-link voltage ( $V_{dc}$ ), solar irradiation ( $G$ )

waveforms during steady state as well as sag/swell, disturbance conditions of the U-FISMHC for test cases as shown in Figs. 13-15.

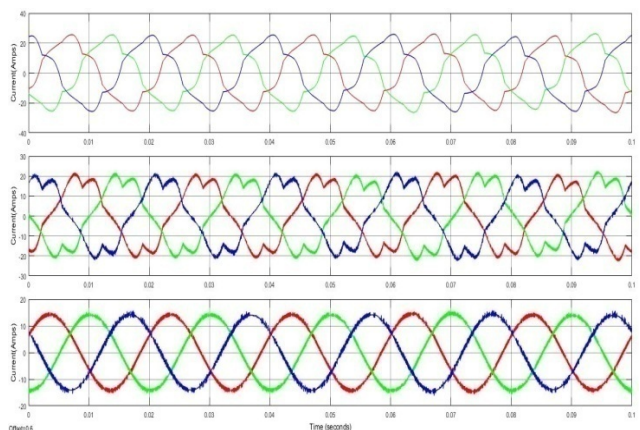
*Case-1:* The supply voltage was considered to be balanced. 30% voltage sag during 0.15-0.25s, 30% voltage swell during 0.35-0.45s and a disturbance during 0.55-0.65s were introduced in the supply voltage. The solar irradiation was considered as  $1000 \text{ w/m}^2$  at constant temperature of  $25^\circ\text{C}$ . The SAPF compensated the grid voltage fluctuations by injecting a suitable  $V_{se}$  to maintain the constant  $V_l$ . The SHAPF compensated the load current harmonics, keeping the grid currents sinusoidal. Fig. 13 shows that the load currents are balanced and non-sinusoidal. It is observed that the THDs of load voltage and source current are (1.57% & 4.64%) and (13.07% & 22.67%) with and without U-FISMHC compensation respectively, and are well within the limits of IEEE-519 standard. The power factor are 0.9979 and 0.7144 for the system with and without proposed UPQC respectively.

*Case-2:* The dynamic behavior of proposed U-FISMHC under solar irradiation variation from  $1000 \text{ w/m}^2$  to  $400 \text{ w/m}^2$  at constant temperature of  $25^\circ\text{C}$  is shown in Fig. 14. As the irradiation decreased, the output voltage of PV reduced from 19V to 8V and the current from 14.87A to 5.95A. The decrease in PV current was supplied by FC and load harmonic suppression was done by the SHAPF. The THD comparison of U-FISMHC with existing techniques for load voltage and source current is given in Fig. 16. Here,  $V_s$  is balanced and  $i_l$  is balanced but non-sinusoidal with high harmonic content. The power factors are 0.9998 and 0.8552 for the system with and without proposed UPQC respectively. It is seen that the power factor is also improved, and the voltage sag/swells and disturbances are compensated with SAPF effectively.

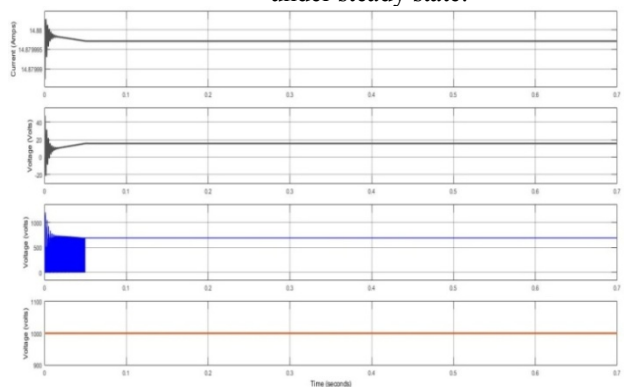
*Case-3:* The dynamic behavior of proposed U-FISMHC for unbalanced supply with irradiation of  $1000 \text{ w/m}^2$  at constant temperature of  $25^\circ\text{C}$  is presented in Fig. 15. Here, the unbalanced supply voltages and the unbalanced load currents were compensated by injecting appropriate compensating voltages and currents to make them sinusoidal. The THDs were well within the standard limits. The resulting power factor after compensation was almost unity. To show the superior performance of proposed scheme, the resulting THDs and power factors are compared with those of the existing PIC, FLC, and SMC in Fig. 16 and Table 5 respectively. It is very clear from the figure and table that the proposed controller is able to provide the best THDs and power factors.



(a) Source voltage, Injected voltage, Load voltage under steady state, sag/swell, disturbance.



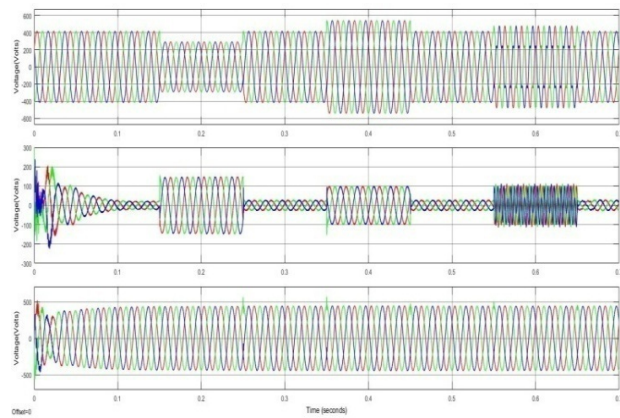
(b) Source current, Injected current, Load current under steady state.



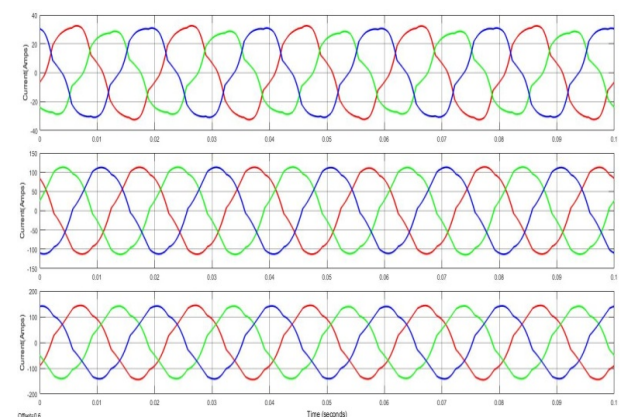
(c) PV panel output current, PV panel voltage , DC-Link Voltage, solar Irradiation

Fig. 13: Waveforms of Proposed system for case-1.

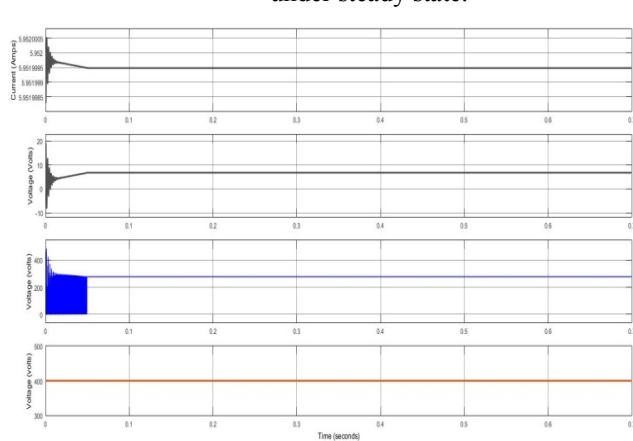
In all case studies the  $V_{dc}$  is maintained constant at 700V, which is shown in part (c) of Figs. 13-15, with settling time of 0.05s and without any overshoot. The settling time of the proposed controller scheme is compared with those of PIC, FLC, and SMC in Table 6, which clearly exhibits that the settling time of the proposed controller scheme is much lower than the other controllers. The FFT analysis of source current for cases 1-3 of the proposed UPQC system are shown in Figs. 17-19 respectively. They clearly exhibit that the THD in all cases are within the IEEE standard limits.



(a) Source voltage, Injected voltage, Load voltage under steady state, sag/swell, disturbance.

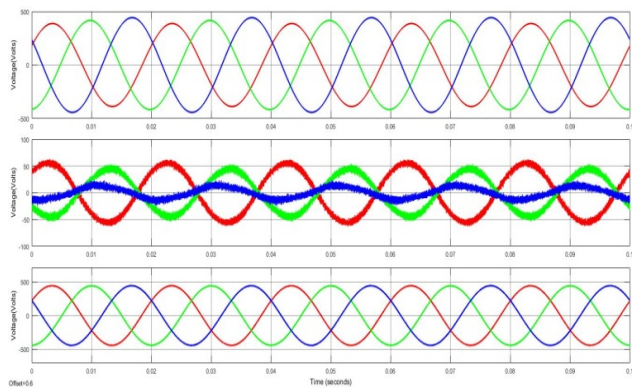


(b) Source current, Injected current, Load current under steady state.

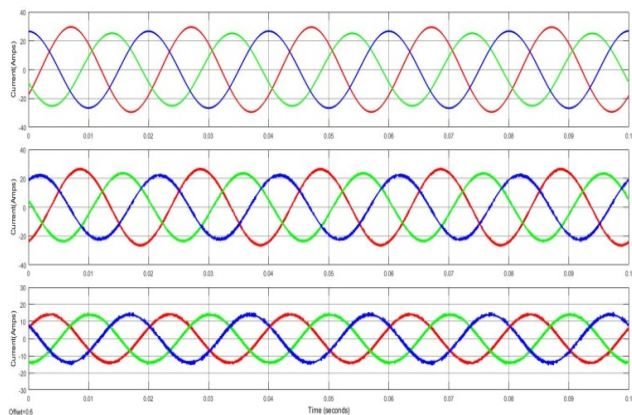


(c) PV panel output current, PV panel voltage , DC-Link Voltage, solar Irradiation

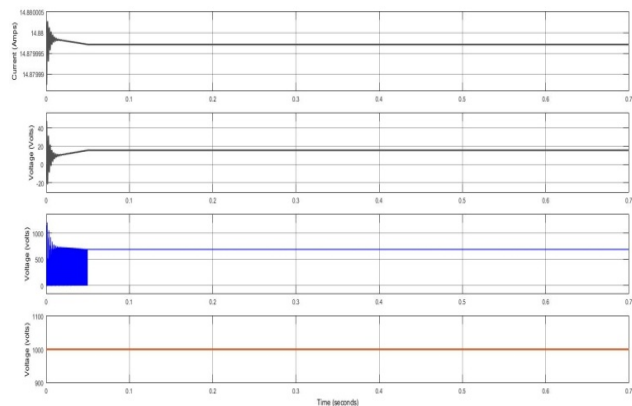
Fig. 14: Waveforms of Proposed system for case-2.



(a) Source voltage, Injected voltage, Load voltage under steady state.



(b) Source current, Injected current, Load current under steady state.



(c) PV panel output current, PV panel voltage , DC-Link Voltage, solar Irradiation

Fig. 15: Waveforms of Proposed system for case-3.

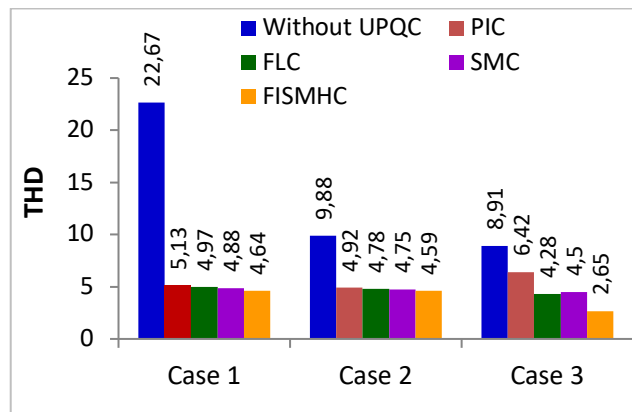


Figure 16: THD Comparison Bar chat

Table 5: Power factor comparison for case studies

Case	Without UPQC	PIC	FLC	SMC	FISMHC
1	0.7144	0.8780	0.9961	0.9951	0.9979
2	0.8552	0.9210	0.9944	0.9954	0.9998
3	0.7399	0.9352	0.9964	0.9954	0.9987

Table 6: Settling time of DC-Link voltages for case studies

Case	PIC	FLC	SMC	FISMHC
1	0.2	0.1	0.07	0.05
2	0.2	0.1	0.08	0.05
3	0.2	0.1	0.07	0.05

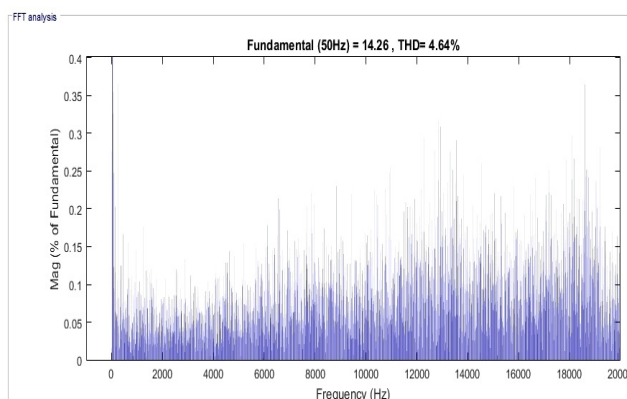


Fig 17: Current THD for Case1

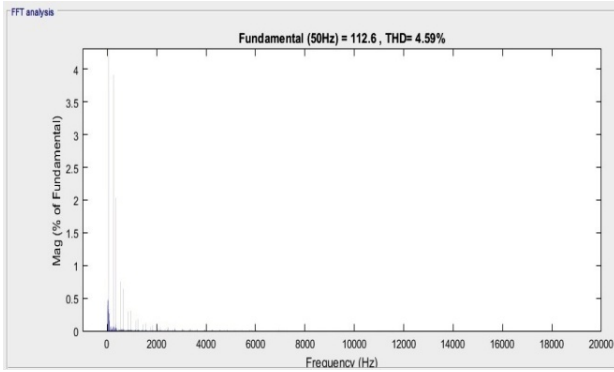


Fig 18: Current THD for Case2

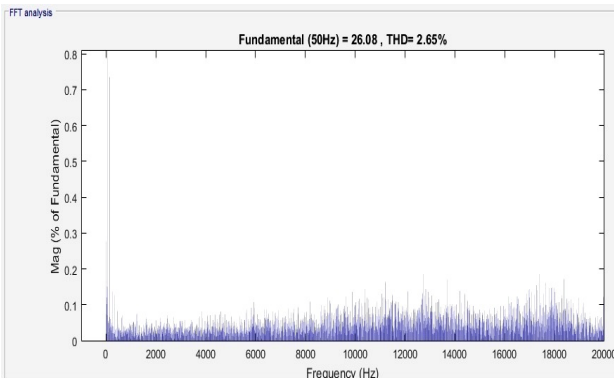


Fig 19: Current THD for Case3

## 5. Conclusion

In this work SS-FC based U-FISMHC has been designed for three-phase distribution systems. Three test cases based on different combinations of solar irradiation, temperature and loads were considered and compared with the PIC, FLC, and SMC for analyzing the performance of the proposed scheme. The results exhibited that the U-FISMHC is the best choice for PQ enhancement. The proposed controller provides lower THD that is well within IEEE standards, maintains almost unity power factor, provides constant DC-Link voltage with minimum settling time, and eliminates voltage fluctuations effectively. It also proves that it can provide compensation for unbalanced supply voltages effectively.

## References

1. H. Fujita, H. Akagi, “The unified power quality conditioner: The integration of series and shunt-active filters”, IEEE Trans. Power Electronics, DOI: 10.1109/63.662847, Vol. 13, No. 2, pp. 315-322, March 1998.
2. Y.Y. Kolhatkar, R.R. Errabelli, S.P. Das, “A sliding mode controller based optimum UPQC with minimum VA loading”, IEEE Power Engineering Society General Meeting, pp. 871–875, June 2005.
3. F. Mekri, M. Machmoum, N.A. Ahmed, B. Mazari, “A fuzzy hysteresis voltage and current control of a unified power quality conditioner”, Industrial Electronics, IECON 34<sup>th</sup> Annual Conference of IEEE, pp. 2684–2689, 2008.
4. V. Khadkikar, A. Chandra, “A new control philosophy for a unified power quality conditioner (UPQC) to coordinate load-reactive power demand between shunt

- and series inverters”, IEEE Transactions on Power Delivery, DOI: 10.1109/TPWRD.2008.921146, Vol. 23, No. 4, pp: 2522–2534, Oct. 2008.
5. V.G. Kinhal, P. Agarwal, H.O. Gupta, “Performance investigation of neural-network-based unified power-quality conditioner”, IEEE Transactions on Power Delivery, DOI: 10.1109/TPWRD.2010.2050706, Vol. 26, No. 1, pp: 431–437, Jan. 2011.
6. A.E. Leon, S.J. Amodeo, J.A. Solsona, M.I. Valla, “Non-linear optimal controller for unified power quality conditioners”, IET Power Electron, Vol. 4, No. 4, pp: 435–446, April 2011.
7. Vinod Khadkikar, “Enhancing Electric Power Quality Using UPQC: A comprehensive Overview”, IEEE Transactions on Power Electronics, DOI: 10.1109/TPEL.2011.2172001, Vol. 27, No. 5, pp. 2284 – 2297, May 2012.
8. S.A. Taher, S.A. Afsari, “Optimal location and sizing of UPQC in distribution networks using differential evolution algorithm”, Mathematical Problems in Engineering, Vol. 12, pp. 1-21, Aug-2012.
9. Salim Chennai, M-T Benchouia, “Unified power quality conditioner based on a three-level NPC inverter using fuzzy control techniques for all voltage disturbances compensation”, Frontiers Energy, Vol. 8, No. 2, pp. 221–239, Jan 2014.
10. B. Gopal, Pannala Krishna Murthy, G. N. Sreenivas, “Power Quality Improvement Using UPQC Integrated with Distributed Generation Network”, International Journal of Electrical and Computer Engineering, DOI: 10.5281/zenodo.1339113, Vol. 8, No.7, 2014.
11. Swapnil Y. Gadgune, Madhukar M. Waware, “A Novel Control Strategy for Capacitor Voltage Regulation of Unified Power Quality Conditioner Using Integral plus Sliding Mode Controller”, International Conference on Circuit, Power and Computing Technologies, 2015.
12. A. Kalair, N. Abas, A.R. Kalair, Z. Saleem, N. Khan, “Review of harmonic analysis, modeling and mitigation techniques”, Renewable and Sustainable Energy Reviews, DOI: 10.1016 / j.rser.2017.04.121, Vol. 78, pp. 1152–1187, Oct-2017.
13. Sarita Samal and Prakash Kumar Hota, “Design and analysis of solar PV-fuel cell and wind energy based microgrid system for power quality improvement”, Cogent Engineering, Vol. 4, No. 1, pp. 1-22, Nov-2017.
14. Tejinder Singh Saggi, Lakhwinder Singh, Balbir Gill & Om Parkash Malik, “Effectiveness of UPQC in Mitigating Harmonics Generated by an Induction Furnace”, Electrical power components and systems, Taylor& Francis, Vol. 46, No. 6, pp. 629-636, Nov-2018.
15. Mojtaba Yavari, Sayyed Hossein Edjtahed, Seyed Abbas Taher, “A non-linear controller design for UPQC in distribution systems”, Alexandria Engineering Journal, Vol. 57, No. 4, pp:3387-3404. Dec-2018.
16. Sudheer Vinnakoti, Venkata Reddy Kota, “Implementation of artificial neural network based controller for a five-level converter based UPQC”, Alexandria Engineering Journal, Vol. 57, No. 3, pp.1475-1488, 2018.

17. Santanu Kumar Dash, Pravat Kumar Ray, "Novel PV-tied UPQC topology based on a new model reference control scheme and integral plus sliding mode dc-link controller", *Int Trans Electrical Energy Systems*, Vol. 28, No. 7, e2564, July-2018.
18. V. Veera Nagireddy, Venkata Reddy Kota, D.V. Ashok Kumar, "Hybrid fuzzy back-propagation control scheme for multilevel unified power quality conditioner", *Ain Shams Engineering Journal*, Vol. 9, No. 4, pp: 2709-2724, Dec- 2018.
19. Sahithullah Mahaboob, Senthil Kumar Ajithan, Sasikala Jayaraman, "Optimal design of shunt active power filter for power quality enhancement using predator-prey based firefly optimization", *Swarm and Evolutionary computation*, Vol. 44, pp. 522-533, Feb- 2019.
20. E. Nandhini & A. Sivaprakasam, "A Review of Various Control Strategies Based on Space Vector Pulse Width Modulation for the Voltage Source Inverter", *IETE Journal Of Research*, May-2020.
21. Muhammad Alif Mansor, Kamrul Hasan, Muhammad Murtadha Othman, "Construction and Performance Investigation of Three-Phase Solar PV and Battery Energy Storage System Integrated UPQC", *IEEE Access*, DOI:10.1109/ACCESS.2020.2997056, Vol. 8, pp. 103511 – 103538, April-2020.
22. N.C.Sai Sarita, S.Suresh Reddy, P.Sujatha, "Control strategies for power quality enrichment in Distribution network using UPQC", *material today proceedings*, July- 2021.
23. Akhil Gupta, "Power quality evaluation of photovoltaic grid interfaced cascaded H-bridge nine-level multilevel inverter systems using D-STATCOM and UPQC", Vol. 23, No. 8, January 2022.
24. K.B.V.S.R. Subrahmanyam, B. Gopal, "PV system integration with multilevel-UPQC for power quality improvement in distribution system", *material today proceedings*, Nov-2020.
25. Sk. Abdul Pasha, N. Prema Kumar, "Analysis of THD in three phase two-bus distribution system by RL & RC – Loads with UPQC", *material today proceedings*, Feb-2021.
26. Shahd Fadhil Jaber, Amina Mahmoud Shakir, "Design and Simulation of a Boost-Microinverter for Optimized Photovoltaic System Performance", *International Journal of Smart Grid*, Vol. 5, No. 2, June 2021.
27. Abilash Thakallapelli, Sudipta Ghosh; Sukumar Kamalasan, "Real-time frequency based reduced order modeling of large power grid" 2016 IEEE Power and Energy Society General Meeting (PESGM) Boston, MA, USA, 17-21 July 2016. (Conference)
28. Ming-Tsung Tsai, Ching-Lung Chu, Wei-Cong Chen, "Implementation of a Serial AC/DC Converter With Modular Control Technology", 2018 7th International Conference on Renewable Energy Research and Applications (ICRERA), Paris, France, 14-17 Oct. 2018.
29. Satoshi Ikeda, Fujio Kurokawa, "Isolated and wide input ranged boost full bridge DC-DC converter for improved resilience of renewable energy systems", 2017 IEEE 6th International Conference on Renewable Energy Research and Applications (ICRERA), San Diego, CA, USA, 5-8 Nov. 2017.
30. Subhransu Sekhar Dash, "Tutorial 1: Opportunities and challenges of integrating renewable energy sources in smart" 2017 IEEE 6th International Conference on Renewable Energy Research and Applications (ICRERA), San Diego, CA, USA, 5-8 Nov. 2017.
31. Koganti Srilakshmi, P. Ravi Babu, P. Aravindhababu, "An enhanced most valuable player algorithm based optimal power flow using Broyden's method", *Sustainable Energy Technologies and Assessments*, DOI: 10.1016/j.seta.2020.100801, Vol. 24, 100801, Dec-2020.
32. Koganti Srilakshmi, P. Ravi Babu, Yogambari Venkatesan, Aravindhababu Palanivelu, "Soccer league optimization for load flow analysis of power Systems", *International Journal of Numerical Modeling*, DOI: 10.1002/jnm.2965, Oct-2021.